Distribution characteristics of gullies with slope gradient in Northeast China

Dichen Wang · Haoming Fan (ID)

Abstract Twenty selected watersheds were divided into five small watershed sets according to location in Liaoning Province (LN), China. Watersheds and slopes were extracted from a 1:50,000 DEM, and gully data for each watershed were obtained by remote sensing interpretation. The gullies and associated slopes within the small watersheds were identified, and the distributions of gully density, proportion of dissected land, and gully length-width ratio in each small LN watershed and in the five small watershed sets were obtained. The correlations between the small watershed sets and the gully distributions throughout LN demonstrate regional distribution differences, and the watershed area has a great influence on both the area and length of gullies. Regional differences are present in the gully density and the proportion of dissected land in the small watersheds. The distribution of gullies with respect to slope depends on both the gully parameters and the proportion of terrain in the different slope grade ranges. The distribution results for the five small watershed sets are similar to those from a census of the Liaoning-Around Bohai mountainous and hilly sub-region. The gully density and proportion of dissected land in LN showed a single-peak curve with respect to slope, with slope thresholds of 8° and 5°, respectively. The constructed distribution equation has a high degree of fit. The comprehensive distributions of gully density, proportion of dissected land, and length-width ratio with slope indicate that gully erosion in LN is serious within the slope range of 3~8°.

Keywords Gully · Distributing · Slope · Density · Proportion of dissected land · Length-width ratio

Introduction

Gullies are ubiquitous topographic features associated with soil erosion worldwide (Capra et al. 2009a; Martineli Costa and de Almeida Prado Bacellar 2007; Rengers and Tucker 2014; Kukal and Bhatt 2014; Sidorchuk et al. 2003). Gullies can be found throughout China, including on the barren Loess Plateau and in the fertile black soil region of Northeast China (Hessel and van Asch 2003; Li et al. 2015; Wang et al. 2017). The development of gullies not only changes the compositional characteristics within and between different land types but also reduces the extent of available arable land, diminishes the crop yield, and increases the amount of labor required to cultivate the land (Valentin et al. 2005). It is estimated that nearly 5% of the time spent on field work in northern Laos each year is allocated to backfilling gullies (Valentin et al. 2005). The same phenomenon is observed in Northeast China, where time and labor are spent either mechanically paving paths across erosion gullies before the harvest or directly replanting crops in gullies after the harvest. The problems associated with gullies have become the subject of

D. Wang · H. Fan (✉)
College of Water Conservancy, Shenyang Agricultural University, No. 120 Dongling Road, Shenhe District, Shenyang City 110866 Liaoning Province, People's Republic of China
e-mail: fanhaoming@163.com

increasing concern for scholars from various countries as a deeper understanding of the dangers they pose has been gained; hence, gullies have become a major topic at international conferences around the globe (Jean Poesen and Valentin 2003; Valentin et al. 2005).

Gullies are generated by the concentrated scouring effects of surface runoff. Erosion can be induced when the runoff magnitude and duration reach a certain extent. Runoff-based erosion can even be sustained (Vandaele et al. 1996). Gullies are a common feature in areas characterized by steep mountains and hilly terrain (Valentin et al. 2005); in particular, numerous mountains and hills are distributed throughout Liaoning Province (LN), China. Compared with gentle slopes, steep slopes are more likely to increase the runoff velocity and to produce gully erosion, although steep slopes generate less runoff (Janeau et al. 2003). Furthermore, larger amounts of runoff are more likely to cause soil compaction, and thus, the slope threshold of a rill may be relatively low (Valentin et al. 1999).

In the past, with the motivation of resolving agricultural problems, many studies have focused on rill and inter-rill erosion. With the attention that is being increasingly directed towards the remote influence of soil erosion, research on rill erosion at the basin scale has gradually become a hot topic (Valentin et al. 2005). A watershed is considered to be a collection of spatial processes with different erosion potentials (Sidorchuk et al. 2003). However, many studies lack sufficient runoff data, and thus, watershed data have been used to replace runoff data (Cheng et al. 2007). In 1975, Patton and Schumm (1975) determined the starting points of erosion gullies on 1:12,000 aerial photographs and established the relationship between the drainage basin and slope based on a topographic map. Meanwhile, an analysis of slope and area data collected in northwestern Colorado found a negative relationship between the drainage basin area and slope (Patton and Schumm 1975). Scholars have defined the relationship between the slope and watershed area as $S = aA^b$, where the indexes a and b are determined by the local environment (Poesen et al. 2003; Vandekerckhove et al. 2000). Montgomery and Dietrich (1988) studied gully erosion caused by shallow sliding and seepage erosion on steep slopes through field measurements in three basins in Oregon and California and observed an inverse relationship between the watershed area and the slope of a gully head (David R. Montgomery and Dietrich 1988). Montgomery et al. also concluded that a threshold exists

between the watershed area and the critical gradient; AS^2 values of 500~4000 m^2 were considered to be the point at which gully erosion was initiated (D. R. Montgomery and Dietrich 1992). Wu and Cheng (2005) used global positioning system (GPS) data to measure the shapes and locations of gullies in a small watershed near Suide, Shaanxi Province, and established the critical relationship for the Loess Plateau ($S = 0.1839\ A^{-0.2385}$). Subsequently, Cheng Hong established another critical relationship, $S = 0.058A^{-0.3}$, after studying the ephemeral gullies in the same watershed (Cheng et al. 2007). In Swaziland, South Africa, the concept of the erosion response unit was used to identify the forms and erosion processes of erosion gullies in the Mbuluzi Basin; accordingly, remote sensing and GIS data were applied to identify areas affected by gully erosion and to estimate the corresponding soil losses (Sidorchuk et al. 2003). In recent years, some scholars have conducted considerable research work to explore the main causes, distributions, and morphological characteristics of gullies (Capra et al. 2009b; Dotterweich 2008; Ionita et al. 2015b; Woodward 1999). In particular, one popular research method is to study the gully distribution with respect to the grade of the slope. Scholars have studied the relationships between the spatial distribution of gullies and the slope threshold in South Africa by dividing the slopes into five classes (0~4°, 5~9°, 10~14°, 15~19°, and >20°). The results showed that gullying was predominant in the slope class of 5~9° and was more pronounced in the slope class of 10~14° than in the steeper slope classes of 15~19° and >20° (Kakembo et al. 2009). Using remote sensing data to monitor the erosion of gully in typical black soil areas in the Kebai area, Heilongjiang Province, Northeast China, it is concluded that as the slope increases, the density of the gully increases first and then decreases; the critical threshold of the slope is 3° (Zhang et al. 2015).

Traditionally, researchers have been more interested in rill and inter-rill erosion (Bagherian Kalat et al. 2018; Patin et al. 2018), whereas gully erosion is ignored in most models, and thus, only a few such models have been developed, e.g., the ephemeral gully erosion model (EGEM) (Giménez et al. 2004). At the same time, the three-dimensional nature of gully erosion is affected by a wide range of factors and processes. Although gully erosion is usually triggered or accelerated by land use changes and/or extreme climatic events (Chaplot et al. 2005a, b), its spatial differences and historical factors,

which are much more difficult to predict, cannot be ignored (Chaplot et al. 2005a). With the development of science and technology, the combined use of remote sensing, geographic information systems, and GPS ("3S" technology) is gradually emerging in the field of soil erosion (Vrieling et al. 2007; He et al. 2014). Although the precision of a remote sensing interpretation is relatively poor compared with that of an interpretation using GPS data and drone imagery (Giménez et al. 2004; Cheng et al. 2007), remote sensing platforms are suitable for the acquisition of data over large spatial scales.

At present, GPS measurements are used in the study of the distribution of erosion channels in small watersheds and are combined with other watershed data for analysis. Large-scale distribution studies are based on remote sensing interpretation. There is a lack of transition between small watershed studies and large regional studies. Therefore, by selecting 20 small watersheds, erosion gullies are identified via remote sensing interpretation, and the differences in the distribution of

erosion gullies between different watersheds are studied. Consequently, this work built the relationship of small-scale and large-scale studies.

Materials and methods

Study area

LN, which covers a total land area of 14.75×10^4 km^2, is located in the southern region of Northeast China (118°53′~125°46′E, 38°43′~43°26′N). LN is bordered to the southwest by Hebei Province, to the northwest by the Inner Mongolia Autonomous Region, and to the northeast by Jilin Province. The study area in LN (Fig. 1) contains a total of 20 small watersheds divided into five sets of watersheds. These five watershed sets are located in Kuandian Manchu Autonomous County (Yong'an, Erlongdu, Guafangzi, and Dajianchang) in the eastern part of LN, Pulandian City (Guling, Xingtai, Guotun, and Diaojia), in the southern part of LN,
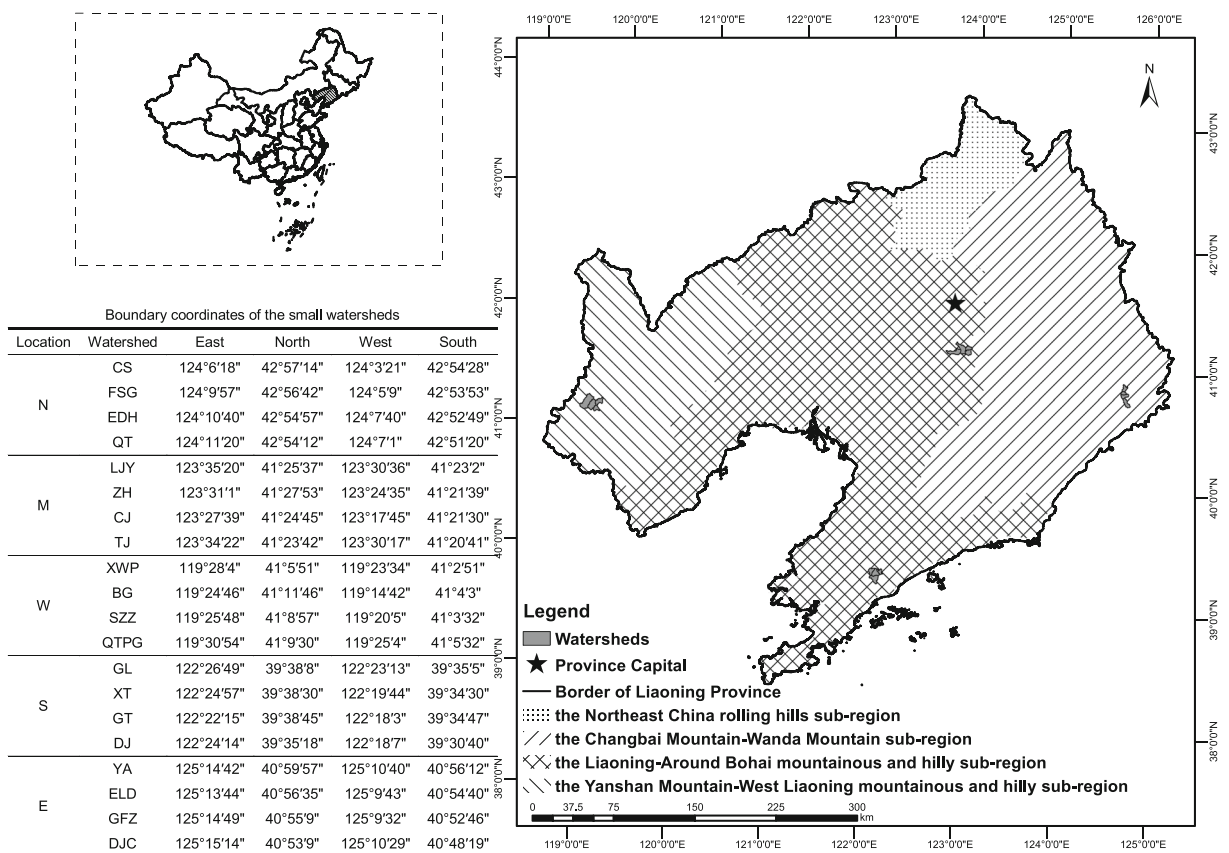

Boundary coordinates of the small watersheds

Location	Watershed	East	North	West	South
N	CS	124°6′18″	42°57′14″	124°3′21″	42°54′28″
	FSG	124°9′57″	42°56′42″	124°5′9″	42°53′53″
	EDH	124°10′40″	42°54′57″	124°7′40″	42°52′49″
	QT	124°11′20″	42°54′12″	124°7′1″	42°51′20″
M	LJY	123°35′20″	41°25′37″	123°30′36″	41°23′2″
	ZH	123°31′1″	41°27′53″	123°24′35″	41°21′39″
	CJ	123°27′39″	41°24′45″	123°17′45″	41°21′30″
	TJ	123°34′22″	41°23′42″	123°30′17″	41°20′41″
W	XWP	119°28′4″	41°5′51″	119°23′34″	41°2′51″
	BG	119°24′46″	41°11′46″	119°14′42″	41°4′3″
	SZZ	119°25′48″	41°8′57″	119°20′5″	41°3′32″
	QTPG	119°30′54″	41°9′30″	119°25′4″	41°5′32″
S	GL	122°26′49″	39°38′8″	122°23′13″	39°35′5″
	XT	122°24′57″	39°38′30″	122°19′44″	39°34′30″
	GT	122°22′15″	39°38′45″	122°18′3″	39°34′47″
	DJ	122°24′14″	39°35′18″	122°18′7″	39°30′40″
E	YA	125°14′42″	40°59′57″	125°10′40″	40°56′12″
	ELD	125°13′44″	40°56′35″	125°9′43″	40°54′40″
	GFZ	125°14′49″	40°55′9″	125°9′32″	40°52′46″
	DJC	125°15′14″	40°53′9″	125°10′29″	40°48′19″

Fig. 1 Study area

Lingyuan City (Xiaowopu, Beigou, Shenzhangzi, and Qiantaipinggou), in the western part of LN, Changtu County (Changsheng, Fangshengou, Erdaohe, and Quantou), in the northern part of LN and Dengta City (Laojunyu, Zhanghai, Cuijia, and Tangjia), and in central LN. The annual average temperature in the study area is 5~10 °C, and the average temperature decreases from the southwest to the northeast from mountainous terrain to plains. The annual sunshine duration is 2270~2990 h, and the average frost-free period is 124~215 days. The average annual precipitation is 400~1200 mm and decreases from southeast to northwest. The largest amount of rainfall occurs in Kuandian Manchu Autonomous County, which experiences an annual precipitation of more than 1200 mm, whereas the minimum amount of rainfall (less than 400 mm) occurs in Jianping County to the northwest. From June to August, rainfall accounts for 60% to 70% of the annual precipitation. The annual average wind speed is 2~4 m/s, which decreases gradually from the coastal regions to the inland regions and from plains to mountainous terrain.

The dominant landform in LN is the Liao River plain, which is surrounded on three sides by the high hills of eastern LN and northern LN and the low hills of western LN. The land area proportions of mountainous terrain, plains, and water bodies are 58%, 33%, and 9%, respectively. The terrain tilts downward towards the center of LN from the north to the south and from the east and west; mountainous hills are roughly distributed along the eastern and western sides, while the middle is occupied by the vast low-elevation Liao River plain. Five counties (cities) are located among four secondary soil and water conservation regionalization regions in China: Kuandian Manchu Autonomous County belongs to the Changbai Mountain-Wanda Mountain sub-region, southern Pulandian District and central Dengta belong to the Liaoning-Around Bohai mountainous and hilly sub-region, western Lingyuan city belongs to the Yanshan Mountain-West Liaoning mountainous and hilly sub-region, and Changtu County belongs to the Northeast China rolling hills sub-region. The soil and water conservation regionalization in China constitute a combination of natural regions and thematic (e.g., geomorphology, soil, and vegetation) regions. This secondary-level zonation reflects the distributions of major landforms and soil erosion, thereby ensuring the relative consistency of the interval and

the maximum difference between intervals (Zhao et al. 2013). Therefore, the choice of these five watershed sets, regardless of whether the typical consideration is geography or soil erosion, can effectively represent LN.

Data acquisition

Data on the small watersheds and gullies in this study were based on the soil erosion census data of LN collected in 2015. The extraction threshold for small watersheds was iteratively established based on a 1:50,000 digital elevation model (DEM) and 845 river basins in LN with an area of more than 50 km^2, and the threshold was then compared with that of a typical small watershed. Finally, the threshold was set to 10,000.

A general investigation of gullies was carried out based on remote sensing images with a resolution of 2 m and a 1:50,000 DEM. Interactive GIS techniques were used to extract information on the length, area, type, longitudinal gradient, and location of the gullies. The steps in these interactive GIS techniques include (1) transforming the projection, (2) correcting the RS images to eliminate band and spot errors, (3) joining and splitting the images, and (4) loading the images into a database. The RS data are then checked through interpretation and field surveys to avoid missing data and errors, and an attribute table and spatial data for each gully can then be successfully created. The gully survey object is a channel with a length of 100~5000 m, which can be clearly identified in a remote sensing image (Wang et al. 2017).

The slopes were divided into nine classes (0~0.25°, 0.25~1.5°, 1.5~3°, 3~4°, 4~5°, 5~8°, 8~15°, 15~25°, and 25~90°), which were derived from the Standard of Water and Soil Conservation in the Black Soil Region (SL-2009). The DEM was analyzed using ArcGIS 10.2 and the 3D Analyst Toolbox. The DEM of the slope was converted into polygons and stored as shapefiles to enable the distributions to be extracted. The small watershed data and gully data were superimposed to ensure that no erosion gullies within the small watershed were statistically lost; subsequently, related parameters, such as the erosion gully length and area, were calculated. These parameters were then superimposed with the slope layer to obtain the gully slope distribution features.

Results

Distribution characteristics of gullies in the small watersheds

A total of 485 gullies were identified among the 20 small watersheds. The area of each small watershed and the parameters of all gullies (i.e., their quantity, length, and area) within each small watershed are shown in Table 1.

Correlation analysis was conducted between the area of each small watershed and the gully parameters (quantity, length, and area) (Table 2). The results reveal no significant correlation between the areas of the small watershed sets which located in S and N and the gully

parameters (quantity, length, and area). The correlations among some of the parameters of the other three small watershed sets are significant. There are no significant correlations between the area of small watershed set located in M and the gully parameters, but the number of gullies is significantly correlated with both the gully length and the gully area ($R = 0.986^*$, $R = 0.975^*$). The gully length and area in small watershed set located in N are significantly correlated ($R = 0.985^*$). Similarly, in the small watershed set located in W, the gully number and length are significantly correlated ($R = 0.968^*$), and the gully length and area are also significantly correlated ($R = 0.981^*$).

All small watersheds are also considered as a whole to analyze the correlation between erosion gully

Table 1 Table of parameters of the small watersheds and gullies

Location	Small watershed	Small watershed area (km^2)	Gully characteristics		
			Number (slip)	Length (m)	Area (km^2)
East (E)	DJC	27.12	26	8003.82	0.08
	ELD	12.31	5	5362.57	0.10
	GFZ	19.36	34	13,433.26	0.20
	YA	18.17	24	10,065.75	0.15
Subtotal		76.96	89	36,865.40	0.52
Middle (M)	CJ	40.73	6	5250.26	0.09
	LJY	17.63	4	3741.58	0.07
	TJ	22.58	11	6171.86	0.10
	ZH	44.46	23	13,850.36	0.25
Subtotal		125.40	44	29,014.05	0.51
North (N)	EDH	9.04	12	2889.74	0.14
	FSG	19.44	18	5435.42	0.18
	QT	10.67	13	2906.32	0.14
	CS	12.92	7	2371.43	0.14
Subtotal		52.06	50	13,602.91	0.61
South (S)	DJ	37.44	46	11,545.93	0.24
	GL	15.47	47	9197.65	0.14
	GT	22.21	31	5637.70	0.06
	XT	31.02	95	13,284.79	0.18
Subtotal		106.14	219	39,666.07	0.2
West (W)	BG	84.43	36	28,635.58	1.72
	QTPG	28.06	23	13,245.74	0.46
	SZZ	44.06	18	6565.11	0.16
	XWP	18.87	6	1841.21	0.06
Subtotal		175.42	83	50,287.64	2.40
Total		535.98	485	169,436.06	4.66

Table 2 Correlation coefficients between the areas of small watersheds and gully parameters

	CA (M)	GN (M)	GL (M)	GA (M)	
CA (E)	–	0.610	0.700	0.708	CA (M)
GN (E)	0.662	–	0.986*	0.975*	GN (M)
GL (E)	0.269	.900	–	0.998**	GL (M)
GA (E)	−0.171	0.624	0.903	–	GA (M)
	CA (E)	GM (E)	GL (E)	GA (E)	
	CA (S)	GN (S)	GL (S)	GA (S)	
CA (N)	–	0.339	0.619	0.706	CA (S)
GN (N)	0.594	–	0.828	0.432	GN (S)
GL (N)	0.866	0.904	–	0.863	GL (S)
GA (N)	0.939	0.819	0.985*	–	GA (S)
	CA (N)	GN (N)	GL (N)	GA (N)	
	CA (W)	GN (W)	GL (W)	GA (W)	
	–	0.881	0.894	0.916	CA (W)
		–	0.968*	0.909	GN (W)
			–	0.981*	GL (W)
				–	GA (W)

CA small watershed area, *GN* gully number, *GL* gully length, *GA* gully area

* Significance level < 0.05, ** Significance level < 0.01

Table 3 Correlation coefficients between the small watershed area and gully parameters

	Catchment area	Gully number	Gully length	Gully area
Catchment area		.259	.801**	.803**
Gully number			.524*	.190
Gully length				.847**
Gully area				

* Significance level < 0.05, ** Significance level < 0.01

parameters and watershed area (Table 3). The results of this analysis differ from the results of a separate analysis for each small watershed. The correlations of the small watershed area with both the erosion gully length and the erosion gully area are highly significant ($R = 0.801**$ and $R = 0.803**$, respectively), indicating that the area of a small watershed greatly affects the lengths and areas of the gullies therein. The number and length of erosion gullies show a significant correlation ($R = 0.524*$); to some extent, this relationship indicates that the number of gullies is not heavily influenced by the gully length. This relationship may be related to the

development of gully branches: during the formation of branches, although the total gully length increases, the number of gullies does not increase, and thus, the gully length and the number of gullies are significantly correlated. Gully length is also significantly correlated with the area ($R = 0.847**$), indicating that the development of the gully length has a strong influence on the magnitude of the gully area.

The distribution and development of gullies are directly reflected in the length, area, and volume, as these factors are closely correlated with each other (Fan et al. 2018). Although the correlation analysis of the length, area, and volume of gullies among the five small watershed sets does not reveal that they are completely significantly correlated, it does not indicate that there is no relationship between gully length and area. In the same way, the regional differences in the gully distribution are also reflected in the correlations between the small watershed sets. Many factors affect the development of a gully (Ionita et al. 2015a; Li et al. 2015). However, a small watershed is actually a catchment area, and the influence of the catchment area on the distribution of gullies therein is thoroughly understood (Cheng et al. 2007; Taguas et al. 2015). The difference in the correlations between the watershed sets and all small watersheds does not mean that there are no correlations between the watershed areas and gully parameters. The data of a small watershed set represent the characteristics of that particular area, whereas the data of all small watersheds represent an entire region. Hence, there are no contradictions in the differences among the correlation analysis results.

Distribution characteristics of gully density along slope gradient

The gully density is one of the most important indicators for studying the gully distribution. The slope is divided into nine grades in this study, and the gully density is obtained for each grade. As shown in Fig. 2, the eastern watershed set does not contain any gullies on slopes of 0~0.25°. Similarly, no gullies are found in the northern watershed set when the slope is greater than 15°, and no gullies are detected in the southern and western watershed sets when the slope is greater than 25°. No gullies are distributed in the northern watershed set when the slope is greater than 25° because the slope in the small watershed is not greater than 25°, leading to the lack of gully development.

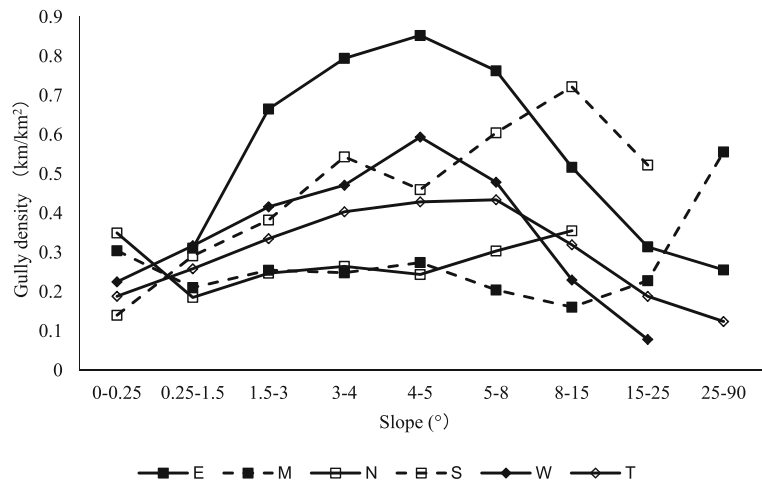**Fig. 2** Distribution of the gully density

Fig. 2 Distribution of the gully density

The densities of the gullies in the northern and middle small watershed sets initially decrease with an increase in the slope gradient and then increase with an increasing slope gradient when the slope gradient exceeds 1.5°. However, the trend of the distribution of the gully density differs between the two sets when the slope exceeds 3°. The gully density in the northern small watershed set continues to rise: when the slope reaches 5°, the gully density decreases by 0.02 km/km^2, and when the slope exceeds 5°, the gully density increases with the slope and ultimately reaches a maximum at 15°. The gully density of the middle small watershed set decreases to 0.24 km/km^2 when the slope is greater than 3° and then increases to 0.27 km/km^2 when the slope reaches 5°. Then, the gully density of the middle small watershed set decreases again with an increasing slope and reaches a minimum when the slope is 15°. When the slope exceeds 15°, the gully density increases with an increasing slope, and it continues to increase until it reaches a maximum at 25~90°.

The densities of the gullies in the eastern and western small watershed sets first increase and then decrease with an increase in the slope gradient, and the maximum gully density is within the slope gradient range of 5~8°. The gully density is 0 km/km^2 when the slope in the eastern small watershed set ranges from 0 to 0.25° because there are no gullies in this slope range. The gully density in the western small watershed set is 0 km/km^2 in the slope range of 25~90° because none of the terrain is steeper than 25° in the western small

watershed set. This also reflects the influences of the differences between the eastern and western topographies on the gully distribution.

The densities of the gullies in the southern small watershed form an M-shaped pattern with increasing slope. When the slope is 0~5°, the gully density first increases and then decreases with increasing slope; then, the density again increases with increasing slope when the slope is 5~15°. When the slope exceeds 15°, the gully density decreases with an increasing slope. The gully density is 0 km/km^2 in the range of 25~90° because no gullies occur in this slope range.

The gully data from the five small watershed sets were integrated with terrain data. The results show that the gully density presents a single-peak curve with an increasing slope gradient. Furthermore, the gully density first increases and then decreases with an increasing slope gradient when the slope gradient exceeds 8° (Wang et al. 2017).

Although the gully density is not related to the proportion of each slope range in the small watershed (Table 4), the influence of the topography on the gully density distribution can be determined by comparing the

Table 4 Correlation between the slope and gully density in the watershed sets

	Small watershed set					
	E	M	N	S	W	T
Pearson	− 0.07	− 0.653	0.389	0.183	− 0.155	− 0.017

* Significance level < 0.05, ** Significance level < 0.01

trend of the gully density distributions among the different small watersheds and the five watershed sets. For slopes of 0~0.25°, the gully densities are higher in the northern and middle small watershed sets than in the other three watershed sets. This pattern is chiefly because the proportions of the slope areas in the northern and middle watershed sets are smaller than those of the gullies within this slope range. The gully density in the middle small watershed set is obviously higher than those in the other small watershed sets in the slope gradient range from 25 to 90°. Although the proportion of the slope gradient (0.16%) and the proportion of the gully length (0.39%) are low, they are different by a factor of 2.44, which is obviously larger than the differences associated with the other slope classes in this small watershed set. Therefore, the distribution of gullies is correlated with the topography.

By collecting all the small watershed gully data and determining the accumulated density of different slopes, we constructed the following distribution equation: $y = 0.1946x^{1.262}$ ($R^2 = 0.9926$), where y is the gully density and x is the slope class.

Distribution characteristics of the proportion of dissected land along the slope gradient

The existence of erosion gullies disrupts the smoothness of the land surface. In this study, the area of gullies per unit area is expressed as the proportion of land dissected by gullies. As shown in Fig. 3, the distribution of dissected land with respect to slope is the same as that of the gully density in the eastern, western, and southern small watershed sets. With an increase in the slope, the proportions of dissected land in the eastern and western small watershed sets

first increase and then decrease, and the maximum value is within the slope range of 5~8°. The proportion of dissected land in the southern small watershed set forms an M-shaped pattern with increasing slope. Specifically, when the slope is between 0° and 4°, the proportion of dissected land first increases, then decreases and increases again with increasing slope. When the slope exceeds 8°, the proportion of dissected land again decreases with increasing slope and becomes 0 in the range of 25~90°.

The proportions of land cut by gullies in the middle and northern small watershed sets first decrease and then increase with increasing slope when the slope reaches 1.5°. The proportion of dissected land increases continuously and reaches the maximum value in the northern small watershed set. When the slope of the central basin is in the range of 0~15°, the proportion of dissected land decreases with increasing slope and then increases again when the slope exceeds 15°.

The gully data from the five watershed sets were again integrated with the terrain data. The results show that the proportion of land cut by gullies increases with the slope gradient, forming a single-peak curve consistent with the gully density distribution curve. The proportion of dissected land first increases and then decreases with the slope gradient, and it increases when the slope gradient is greater than 5°.

By collecting all the small watershed gully data and determining the accumulated proportion of dissected landproportion of dissected land associated with different slopes, we constructed the following distribution equation: $y = 0.356x^{1.4824}$ ($R^2 = 0.9848$), where y is the proportion of dissected land proportion of dissected land and x is the slope class.

Fig. 3 Distribution of the proportion of land cut by gullies
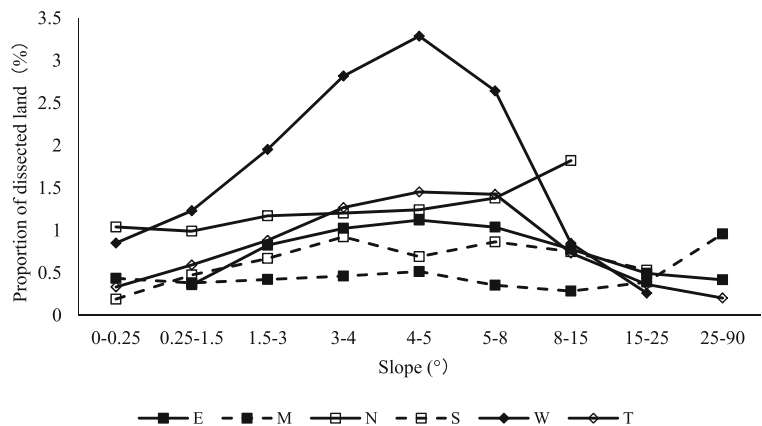
Distribution characteristics of the gully length-width ratio along the slope gradient

The ratio of the length to the width is often used to represent the morphological characteristics of gullies on a certain slope. The larger the ratio of the length to the width, the longer and thinner the gully is. Figure 4 demonstrates that the length-width ratios of the gullies in each small watershed set change repeatedly with increasing slope and form three distributions.

Within the slope range of 0~1.5°, the gullies of the northern small watershed set change from long and thin to short and wide and then transition back to long and thin. The gullies are short and wide on slopes between 3° and 5° but achieve the highest length-width ratios at 8°, beyond which the gullies again become short and wide.

The gullies in the other four small watershed are shortest and widest in conjunction with the minimum slope. As the slope increases, the gullies gradually change from short and wide to long and thin upon reaching the first slope threshold. Although only one threshold exists in the western small watershed set, two slope thresholds exist in the eastern, middle, and southern small watershed sets. The southern small watershed set displays the first gradient threshold at 1.5°, while the other three sets present their first gradient threshold (the only one in the western small watershed set) at 3°. In these small watershed sets, when the slope is 5°, the gullies transition from being short and wide to being long and thin. The gullies in the eastern, middle, and southern small watershed sets reach their longest and thinnest forms

at their second slope thresholds of 25°, 25°, and 15°, respectively. However, the gullies in the western small watershed set do not change after reaching their longest and thinnest state at 25° because the western watershed set has no terrain with a slope exceeding 25°. The trend of the length-width ratio in each of the five small watershed sets is the same as that of the southern small watershed set.

Discussion

Through this study, we can identify the relationship between the slope and the distribution of erosion gullies. In some watershed sets, the changes in the distributions of the gully density, the proportion of dissected land, and the length-width ratio with increasing slope are the same. Furthermore, there are also differences in the distributions among the different watershed sets, thereby reflecting spatial differences (Chaplot et al. 2005a). The five watershed sets were selected from four secondary regions within two primary soil and water conservation regions (i.e., the Northeast China black soil region and the North China mountainous region) in China. The principle of soil and water conservation regionalization reflects the relative consistency within a given region and the relative differences among different regions based on their soil and water loss patterns and topographic and geologic characteristics, and secondary-level regionalization can better reflect the regional characteristics on the basis of first-level regionalization (Zhao et al. 2013). Many

Fig. 4 Length-width ratio distribution of gullies
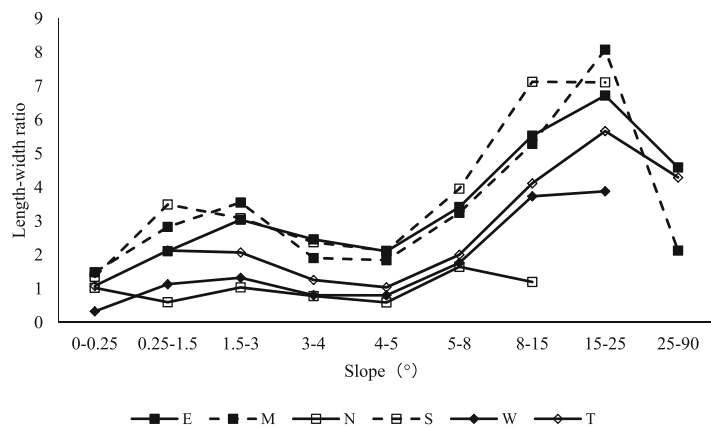
factors affect the development of gullies. Improper farming and irrigation systems, overgrazing, deforestation, road construction, and urbanization can all cause the formation of gullies to varying extents (Valentin et al. 2005). Daily rainfall and soil moisture also represent important factors that affect gully formation, even if the gullies are all within cultivated land (Vandekerckhove et al. 2000). The southern small watershed set is close to the Bohai Sea, while the eastern small watershed set is close to the Yalu River and the Yellow Sea; hence, the rainfall therein is greater than that in the other three sets. Variability in rainfall can change the rainfall erosivity and soil erodibility (Vandekerckhove et al. 2000). Moreover, the impacts of land use differences on gullies are expected to be greater than those of climate differences (Valentin et al. 2005). However, there are more woodlands in the eastern small watershed set, and the western small watershed set is close to Inner Mongolia, China, where there is a certain degree of animal husbandry. For example, the Poike Peninsula began to exhibit large erosion gullies in the twentieth century with an increase in the number of sheep (Mieth and Bork 2005). Differences in the topographic slope also have different influences on runoff (Janeau et al. 2003), thereby affecting the slope threshold of gully formation (Valentin et al. 1999). The southern small watershed set is located in the Northeast China rolling hills sub-region, where the slopes in this sub-region are long and gentle. The other four small watershed sets are all located in mountainous and hilly areas, although the middle small watershed set is located at the edge of the Liaohe Plain. Accordingly, the different landforms in the watershed sets also have varying impacts on the distributions of gullies therein. Differences in topographic and meteorological conditions can also affect vegetation growth and development, and different vegetation types play different roles in delaying the development of gullies (Chen and Cai 2006).

The differences in the gully distribution among the watershed sets are obvious. However, when the adjacent small watersheds are grouped into larger watershed sets or even when the data from different watershed sets are merged, the distributions become more consistent and more similar to the results of a general survey in the Liaoning-Around Bohai mountainous and hilly sub-region (Wang et al. 2017). Therefore, the results of this study can effectively represent the distribution characteristics of gullies in LN.

Conclusion

Each watershed set in this study has its own distribution characteristics in terms of the gully density, the proportion of dissected land and the gully length-width ratio. The distribution of gullies with respect to the slope depends on both the gully parameters and the proportion of terrain in the slope grade ranges.

The gully density and the proportion of land dissected by gullies in Liaoning Province showed single-peak curves with increasing slope, with slope thresholds of 8° and 5°, respectively. The constructed distribution equations have a high degree of fit.

The length-width ratio of each small watershed set changes repeatedly with increasing slope. However, an analysis of the gully density and the proportion of dissected land revealed that the gully density and proportion of dissected land are larger in the slope range of 3~8° and that the length-width ratio is small in this slope range. Therefore, many relatively short gullies are located within this slope range and that gully erosion is serious.

References

Bagherian Kalat, A., Lashkaripour, G. R., Ghafoori, M., & Abbasi, A. A. (2018). Analysis of environmental factors affecting variation in Interrill Erosion under rainfall simulation. *Polish Journal of Environmental Studies, 27*(4), 1573–1581. https://doi.org/10.15244/pjoes/77079.

Capra, A., Porto, P., & Scicolone, B. (2009a). Relationships between rainfall characteristics and ephemeral gully erosion in a cultivated catchment in Sicily (Italy). *Soil and Tillage Research, 105*(1), 77–87. https://doi.org/10.1016/j.still.2009.05.009.

Capra, A., Di Stefano, C., Ferro, V., & Scicolone, B. (2009b). Similarity between morphological characteristics of rills and ephemeral gullies in Sicily, Italy. *Hydrological Processes, 23*(23), 3334–3341. https://doi.org/10.1002/hyp.7437.

Chaplot, V., Coadou le Brozec, E., Silvera, N., & Valentin, C. (2005a). Spatial and temporal assessment of linear erosion in catchments under sloping lands of northern Laos. *Catena, 53*, 167–184. https://doi.org/10.1016/j.catena.2005.06.003.

Chaplot, V., Giboire, G., Marchand, P., & Valentin, C. (2005b). Dynamic modelling for linear erosion initiation and development under climate and land-use changes in northern Laos. *Catena, 63*, 318–328. https://doi.org/10.1016/j.catena.2005.06.008.

Chen, H., & Cai, Q. (2006). Impact of hillslope vegetation restoration on gully erosion induced sediment yield. *Science in China Series D, 49*(2), 176–192. https://doi.org/10.1007/s11430-005-0177-4.

Cheng, H., Zou, X., Wu, Y., Zhang, C., Zheng, Q., & Jiang, Z. (2007). Morphology parameters of ephemeral gully in characteristics hillslopes on the loess plateau of China. *Soil and Tillage Research, 94*(1), 4–14. https://doi.org/10.1016/j.still.2006.06.007.

Dotterweich, M. (2008). The history of soil erosion and fluvial deposits in small catchments of Central Europe: Deciphering the long-term interaction between humans and the environment - a review. *Geomorphology, 101*(1–2), 192–208. https://doi.org/10.1016/j.geomorph.2008.05.023.

Fan, H., Wang, Y., Fan, X., & Liu, J. (2018). The characteristics of gulley development in the snow-melting period of typical watersheds in the black soil region of Northeast China. *SWCC*, (5), 64–68. https://doi.org/10.14123/j.cnki.swcc.2018.0127.

Giménez, R., Planchon, O., Silvera, N., & Govers, G. (2004). Longitudinal velocity patterns and bed morphology interaction in a rill. *Earth Surface Processes and Landforms, 29*(1), 105–114. https://doi.org/10.1002/esp.1021.

He, F., Wang, T., Gu, L., Li, T., Jiang, W., & Shao, H. (2014). An integrated use of topography with RSI in gully mapping, Shandong peninsula, China. *ScientificWorldJournal, 2014*, 827124–827129. https://doi.org/10.1155/2014/827124.

Hessel, R., & van Asch, T. (2003). Modelling gully erosion for a small catchment on the Chinese loess plateau. *Catena, 54*(1–2), 131–146. https://doi.org/10.1016/s0341-8162(03)00061-4.

Ionita, I., Niacsu, L., Petrovici, G., & Blebea-Apostu, A. M. (2015a). Gully development in eastern Romania: A case study from Falciu Hills. *Natural Hazards, 79*(S1), 113–138. https://doi.org/10.1007/s11069-015-1732-8.

Ionita, I., Fullen, M. A., Zgłobicki, W., & Poesen, J. (2015b). Gully erosion as a natural and human-induced hazard. *Natural Hazards, 79*(S1), 1–5. https://doi.org/10.1007/s11069-015-1935z.

Janeau, J. L., Bricquet, J. P., Planchon, O., & Valentin, C. (2003). Soil crusting and infiltration on steep slopes in northern Thailand. *European Journal of Soil Science, 54*, 543–553.

Kakembo, V., Xanga, W. W., & Rowntree, K. (2009). Topographic thresholds in gully development on the hillslopes of communal areas in Ngqushwa local municipality, eastern cape, South Africa. *Geomorphology, 110*(3–4), 188–194. https://doi.org/10.1016/j.geomorph.2009.04.006.

Kukal, S., & Bhatt, R. (2014). Extent, distribution and patterns of gully erosion in lower Shiwaliks of Punjab, India. *Environment & Ecology, 32*(2), 401–404.

Li, Z., Zhang, Y., Zhu, Q., He, Y., & Yao, W. (2015). Assessment of bank gully development and vegetation coverage on the Chinese loess plateau. *Geomorphology, 228*, 462–469. https://doi.org/10.1016/j.geomorph.2014.10.005.

Martineli Costa, F., & de Almeida Prado Bacellar, L. (2007). Analysis of the influence of gully erosion in the flow pattern of catchment streams, southeastern Brazil. *Catena, 69*(3), 230–238. https://doi.org/10.1016/j.catena.2006.05.007.

Mieth, A., & Bork, H.-R. (2005). History, origin and extent of soil erosion on Easter Island (Rapa Nui). *Catena, 63*(2–3), 244–260. https://doi.org/10.1016/j.catena.2005.06.011.

Montgomery, D. R., & Dietrich, W. E. (1988). Where do channels begin? *Nature, 336*(6196), 232–234. https://doi.org/10.1038/336232a0.

Montgomery, D. R., & Dietrich, W. E. (1992). Channel initiation and the problem of landscape scale. *Science, 255*(5046), 826–830. https://doi.org/10.1126/science.255.5046.826.

Patin, J., Mouche, E., Ribolzi, O., Sengtahevanghoung, O., Latsachak, K. O., Soulileuth, B., Chaplot, V., & Valentin, C. (2018). Effect of land use on interrill erosion in a montane catchment of northern Laos: An analysis based on a pluri-annual runoff and soil loss database. *Journal of Hydrology, 563*, 480–494. https://doi.org/10.1016/j.jhydrol.2018.05.044.

Patton, P. C., & Schumm, S. A. (1975). Gully Erosion, northwestern Colorado: A threshold phenomenon. *Geology, 3*(2), 88. https://doi.org/10.1130/0091-7613(1975)3<88:gencat>2.0.co;2.

Poesen, J., & Valentin, C. (2003). Gully erosion and global change. [special issue]. *Catena, 50*(2–4), 87–564.

Poesen, J., Nachtergaele, J., Verstraeten, G., & Valentin, C. (2003). Gully erosion and environmental change: Importance and research needs. *Catena, 50*(2–4), 91–133. https://doi.org/10.1016/s0341-8162(02)00143-1.

Rengers, F. K., & Tucker, G. E. (2014). Analysis and modeling of gully headcut dynamics, north American high plains. *Journal of Geophysical Research: Earth Surface, 119*(5), 983–1003. https://doi.org/10.1002/2013jf002962.

Sidorchuk, A., Marker, M., Moretti, S., & Rodolfi, G. (2003). Gully erosion modelling and landscape response in the Mbuluzi River catchment of Swaziland. *Catena, 50*, 507–525.

Taguas, E. V., Guzmán, E., Guzmán, G., Vanwalleghem, T., & Gómez, J. A. (2015). Characteristics and importance of rill and gully erosion: a case study in a small catchment of a marginal olive grove. *Cuadernos de Investigación Geográfica, 41*(1), 107. https://doi.org/10.18172/cig.2644.

Valentin, C., d'Herbe's, J. M., & Poesen, J. (1999). Soil and water components of banded vegetation patterns. *Catena, 37*, 1–24.

Valentin, C., Poesen, J., & Li, Y. (2005). Gully erosion: Impacts, factors and control. *Catena, 63*(2–3), 132–153. https://doi.org/10.1016/j.catena.2005.06.001.

Vandaele, K., Poesen, J., Govers, G., & Wesemael, B. v. (1996). Geomorphic threshold conditions for ephemeral gully incision. *Geomorphology, 16*(2), 161–173. https://doi.org/10.1016/0169-555x(95)00141-q.

Vandekerckhove, L., Poesen, J., Wijdenes, D. O., Nachtergaele, J., Kosmas, C., Roxo, M. J., et al. (2000). Thresholds for gully initiation and sedimentation in Mediterranean Europe. *Earth Surface Processes and Landforms, 25*, 1201–1220.

Vrieling, A., Rodrigues, S. C., Bartholomeus, H., & Sterk, G. (2007). Automatic identification of erosion gullies with ASTER imagery in the Brazilian Cerrados. *International Journal of Remote Sensing, 28*(12), 2723–2738. https://doi.org/10.1080/01431160600857469.

Wang, D., Fan, H., & Fan, X. (2017). Distributions of recent gullies on hillslopes with different slopes and aspects in the black soil region of Northeast China. *Environmental Monitoring and Assessment, 189*(10), 508. https://doi.org/10.1007/s10661-017-6221-y.

Woodward, D. E. (1999). Method to predict cropland ephemeral gully erosion. *CATENA, 37*(3–4), 393–399. https://doi.org/10.1016/S0341-8162(99)00028-4.

Wu, Y., & Cheng, H. (2005). Monitoring of gully erosion on the loess plateau of China using a global positioning system. *Catena, 63*(2–3), 154–166. https://doi.org/10.1016/j.catena.2005.06.002.

Zhang, S. W., Li, F., Li, T. Q., Yang, J., Bu, K., Chang, L., et al. (2015). Remote sensing monitoring of gullies on a regional scale: A case study of Kebai region in Heilongjiang Province, China. *Chinese Geographical Science, 25*(5), 602–611. https://doi.org/10.1007/s11769015-0780-z.

Zhao, Y., Wang, Z., Sun, B., Zhang, C., Ji, Q., Feng, L., & Shi, M. (2013). A study on scheme of soil and water conservation regionalization in China. *Journal of Geographical Sciences, 23*(4), 721–734. https://doi.org/10.1007/s11442-013-1040-8.